

Fidelity of an Optical Memory Based on Stimulated Photon Echoes

M. U. Staudt,¹ S. R. Hastings-Simon,¹ M. Nilsson,¹ M. Afzelius,¹ V. Scarani,¹ R. Ricken,² H. Suche,² W. Sohler,² W. Tittel,^{1,*} and N. Gisin¹

¹*Group of Applied Physics, University of Geneva, CH-1211 Geneva 4, Switzerland*

²*Angewandte Physik, University of Paderborn, 33095 Paderborn, Germany*

(Received 26 September 2006; published 14 March 2007)

We investigated the preservation of information encoded into the relative phase and amplitudes of optical pulses during storage and retrieval in an optical memory based on stimulated photon echo. By interfering photon echoes produced in a single-mode Ti:Er:LiNbO₃ waveguide, we found that decoherence in the medium translates only as loss and not as degradation of information. We measured a visibility for interfering echoes close to 100%. These results may have important implications for future long-distance quantum communication protocols.

DOI: 10.1103/PhysRevLett.98.113601

PACS numbers: 42.50.Md, 03.65.Yz, 42.25.Hz

Transfer of coherence properties between light and atoms can be investigated through interferometric and spectroscopic techniques. These studies are of fundamental interest, but also yield important information for future applications in the field of quantum information science.

In quantum communication schemes, such as quantum cryptography, nonorthogonal states of light are used as information carriers. The encoding of information into the relative phase and amplitudes of a time-bin qubit has proven to be well suited for transmission over long distances, because this coding is robust to the decoherence mechanism in optical fibers [1,2]. However, the extension of quantum communication to arbitrary distances relies on the availability of quantum memories, which are key to the building of a quantum repeater [3]. Although significant progress has recently been reported [4–6], coherent, reversible transfer of quantum information from photons to atoms with high fidelity and efficiency remains an important and open challenge.

From this perspective, it is important to understand how the fidelity of a time-bin qubit evolves when the information is stored in a quantum memory. This is the primary objective of this Letter. In particular, we show a case in which the decoherence in the atomic medium is a state-independent coupling with the environment: its effect on the retrieved signal is therefore only loss, i.e., a decrease of the retrieval probability. By postselecting only cases when photons are actually emitted, one retrieves uncorrupted information, which does not require complicated classical or quantum error correction.

We work in the framework of a recent proposal [7], and of first experimental studies [8], for storage of time-bin qubits based on controlled, reversible, inhomogeneous broadening (CRIB). CRIB is a novel photon-echo type approach, where the inhomogeneous broadening, and the related de- and rephasing are engendered by externally controlled electric fields. Assuming unity absorption probability, a recall efficiency of 100% has been predicted [7,9,10]. Standard photon echoes employ optical pulses for

rephasing, and their efficiency is therefore limited to a few percent. Photon echoes are well known for storage of classical optical pulses [11,12] as well as for being a phase-preserving process. However, the storage of information encoded in the amplitudes and relative phases of subsequent optical pulses, which is crucial for time-bin qubit storage using CRIB, has received only limited attention so far [13,14].

The photon-echo experiments reported here were done using an Er³⁺ doped LiNbO₃ crystal with a waveguiding structure. To our knowledge, these are the first reported photon-echo experiments in Er³⁺:LiNbO₃ waveguides, LiNbO₃ being widely used as a nonlinear material in integrated optics. In the experimental setup the light is guided entirely through standard telecommunication fibers, integrated intensity and phase modulators, polarization controllers, and the Ti-indiffused Er³⁺:LiNbO₃ waveguide in a monomode structure, thus the assumption of a one-dimensional model, often used in theoretical calculations, is fully justified.

A common approach to storage and retrieval of light using photon echoes is based on three-pulse photon echo (3PE), also known as stimulated photon echo [12]. In this process a first strong optical “write” pulse excites the medium, creating an atomic coherence. The “data” pulses, a sequence of pulses encoding the information to be stored, are sent into the medium some time after the write pulse, which transfer the coherence into a frequency-dependent population grating in the ground and excited states. To retrieve the information, a third strong “read pulse” is used, which scatters off the grating and causes a photon echo to be emitted a time after the read pulse, which is equal to the time separation between write and data pulse. If certain conditions for excitation energy and absorption depths are met, the echo is to a high degree an amplitude and phase replica of the stored data pulses. This simplified picture of a population grating is sufficient to describe our experiment, although remaining atomic coherences were a source of additional 2-pulse echoes.

However, these echoes appear at different times compared to the 3PE and could be discarded via time-resolved detection.

Now, consider a data field consisting of two pulses (D_1 and D_2) with an amplitude ratio R and relative phase φ [see Fig. 1(a)]. The 3PEs appear at times $t_e = t_r + t_{D_i} - t_w$ ($i = 1, 2$), where t_r is the time of readout, t_{D_i} the time of data pulse D_i ($i = 1, 2$), and t_w the arrival time of the write pulse. The echoes will thus be $dt = t_{D2} - t_{D1}$ apart.

Because the efficiency of the 3PE is at best a few percent [15], much of the frequency-dependent population grating is preserved in the atomic ensemble after the read pulse. Therefore more echoes can be produced by sending in several read pulses. In our experiment, two subsequent read pulses were used to produce two copies of the data pulse. If we chose the distance between the read pulses to be dt , the same as the distance between the two data pulses D_1 and D_2 , the echo of the second data pulse readout by the first read pulse ($D_2|R_1$), and the echo of the first data pulse readout by the second read pulse ($D_1|R_2$), will be indistinguishable and thus interfere [Fig. 1(c)]. The phase of a 3PE is controlled by the phase of the write, the data, and the read pulse. The write pulse has a phase α_1 , the data pulse phases α_2 and α_3 , and the read pulse phases α_4 and α_5 . Thus one can obtain constructive or destructive interferences by carefully choosing the different phases of the input pulses [16]. This is true provided that the phase or amplitude coherence is not lost partially or totally during storage and retrieval. Note that the experiment can also be described as a correlation measurement [12] between the electric field describing the data pulses, and the read pulses, respectively.

The data pulse above is related to a time-bin qubit. A time-bin qubit [1] is a coherent superposition of a photon being in two time bins, separated by a time difference long

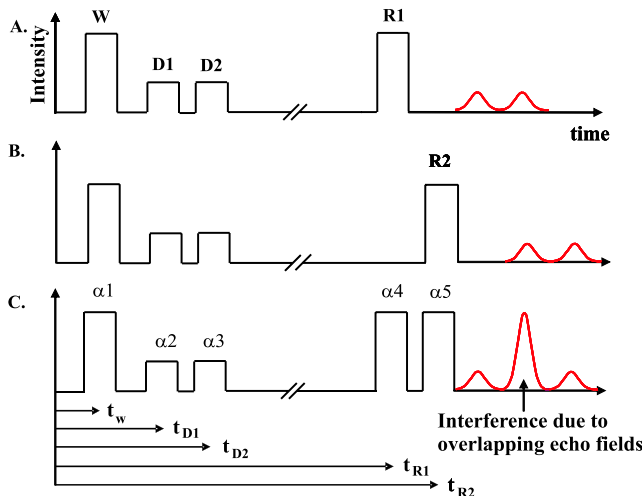


FIG. 1 (color online). Illustration of the sequence of pulses for the interference of photon echoes. The data are read out twice and the phase between data (or read pulses) is changed to produce interference in the central time bin (see text for details).

compared to the coherence time of the photon. It can be written as $|\psi\rangle = c_0|1, 0\rangle + c_1 e^{i\varphi}|0, 1\rangle$, where $|1, 0\rangle$ ($|0, 1\rangle$) stands for a photon being in the first (respectively, the second) time bin and $\varphi = \alpha_2 - \alpha_3$ for the relative phase.

In the present experiment classical coherent pulses were used [see Fig. 1(c)]. These time-bin pulses are two coherent pulses with width smaller than the temporal spacing dt between the two pulses; the state of light is a Poisson distribution of photons ($n \sim 10^8$), each of which is in the state described above.

The output field amplitude of a 3PE, taking $t_w = 0$ and assuming that the whole storage process takes place on a time scale small compared to the radiative lifetime, will be reduced by a factor of e^{-2t_{Dj}/T_2} , where T_2 is the atomic decoherence time. Therefore a time-bin qubit absorbed by a photon-echo material will be emitted as follows, assuming that the photon-echo amplitude is linear as a function of the input field

$$|\Psi\rangle \sim [e^{-2t_{D1}/T_2}c_0|1, 0\rangle + e^{-2t_{D2}/T_2}c_1 e^{i\varphi}|0, 1\rangle]|\mathcal{E}_0\rangle + \lambda|0, 0\rangle|\mathcal{E}_1\rangle. \quad (1)$$

Here $|\mathcal{E}_0\rangle$ and $|\mathcal{E}_1\rangle$ are the states of the environment to which the memory couples and λ reflects the strength of the coupling to state $|\mathcal{E}_1\rangle$. The information encoded in the time-bin qubit is preserved provided $dt = t_{D2} - t_{D1} \ll T_2$ and provided the process has not modified the pulse in such a way that the width of the echo is $\sim dt$. Indeed in this case Eq. (1) can be simplified to $|\Psi\rangle \sim e^{-2t_{D1}/T_2}|\psi\rangle|\mathcal{E}_0\rangle + \lambda|0, 0\rangle|\mathcal{E}_1\rangle$. It follows that even if atomic decoherence has acted during a long time ($t_{D1} \sim T_2$) it does not influence the amplitude ratio or phase difference of the time-bin information. By means of postselecting the cases where a detection is obtained one can thus reach a very high fidelity, however at the expense of a smaller retrieval probability as compared to simply detecting the vacuum component.

The retrieved time-bin pulses (photon-echoes) shown schematically in Fig. 1(c) interfere constructively or destructively depending on the phase difference φ and the phases of the read pulses. The visibility V of the interference should only be a function of the relative amplitudes of the incoming time-bin pulses: $V = 2\sqrt{R}/(1 + R)$ with ratio $R = c_0^2/c_1^2$.

Note that one could also describe our experiment as a setup containing two interferometers, as used for phase-coding quantum cryptography [2]: One interferometer prepares the time-bin qubits, i.e., here our two data pulses, while the second allows the projection measurement, i.e., our two read pulses.

Now we describe the experimental setup, which is similar to the one used in [17]. The output from an external-cavity cw diode laser (Nettest Tunics Plus) was gated by a combined phase and intensity modulator, followed by an intensity modulator (both fiber optic, from Avanex). The first modulator created the five excitation pulses and applied phase shifts to some of the pulses, depending on the

particular experiment, the second modulator was synchronized to the first one and used to improve the peak-to-background intensity ratio. The pulses had durations of $t_{\text{pulse}} = 15 \text{ ns}$, with a clock frequency of 30 Hz. The first data pulse was created at $t_{D1} = 0.6 \mu\text{s}$, the time between the data pulses was typically $dt = 60 \text{ ns}$ and the readout pulses were delayed with regard to the data pulses by 1 to 2 μs . The pulses were then amplified by an EDFA (erbium doped fiber amplifier). To obtain a good background suppression ($>70 \text{ dB}$) and to avoid spectral hole burning by the EDFA, we placed an additional acousto-optical modulator between the optical amplifier and the input of the pulse-tube cooler, which opened only for the series of pulses and suppressed light for all other times. The light was then coupled into the Er^{3+} -doped LiNbO_3 crystal inside the pulse-tube cooler (Vericold), where the crystal was cooled to about 3.4 K. The resulting peak powers were in the range of 5 mW for the write pulses at the refrigerator input (and on the order of 1 mW for the other pulses). The photon echo was detected by a fast detector (1611v, New Focus) after the pulse-tube cooler.

The z-cut LiNbO_3 was erbium doped over a length of 10 mm by indiffusion of an evaporated 8 μm thick Er layer at 1130 °C for 150 h, leading to a Gaussian concentration profile of 8.2 μm 1/e penetration depth and $3.6 \times 10^{19} \text{ cm}^{-3}$ surface concentration. The guiding channel was fabricated by indiffusion of a 7 μm wide, 98 nm thick Ti stripe at 1060 °C for 8.5 h, leading to a monomode guide with a mode size of $4.5 \times 3 \mu\text{m}$ FWHM intensity distribution [18]. The light was injected and collected with standard optical fibers into a waveguide of a diameter of 9 μm . A magnetic field of about 0.2 Tesla was applied parallel to the C_3 axis. This reduces decoherence due to spectral diffusion [19], resulting in a decoherence time of about $T_2 \sim 6 \mu\text{s}$.

Figure 2 shows typical interference patterns for constructive and destructive interference. Here the input data pulses had the same amplitude, thus $R = 1$. We scanned the phase difference between the two interfering photon echoes continuously by varying phase α_2 using the intensity-phase modulator and obtained a clear modulation of the photon-echo interference signal (see Fig. 2).

To extract the visibility we measured the background-subtracted area under the echo interference, and plotted the area as a function of the applied phase. The background was obtained by fitting the signal on either side of the side peaks. We have verified by several measurements, that the detection background was of purely electronic origin and that no coherent or incoherent background light was interfering with the echoes.

We also observed that the side peaks were modulated (see Fig. 2), which we found to be due to an interference between the 3PE with a higher-order echo produced by four excitation pulses (4PE) [20]. The 4PE detected is much smaller than the 3PE, which results into a smaller visibility as compared to pure 3PE interference (see inset in

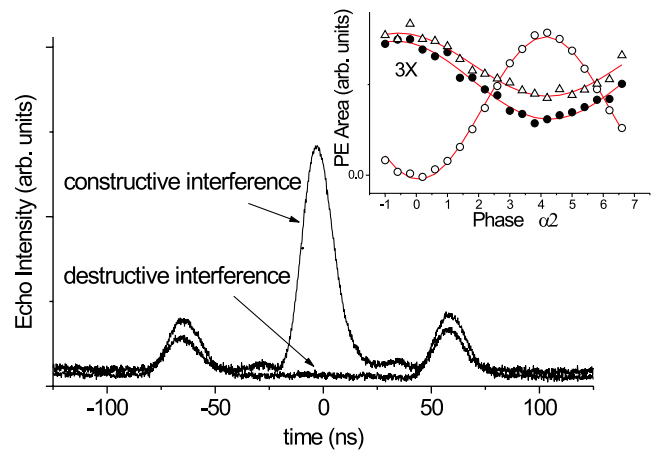


FIG. 2 (color online). Photon-echo signals for constructive and destructive interference. Inset: Central echo area \circ , left \bullet and right Δ side echo area as a function of phase. The phase modulation of both side peaks is synchronized and is opposite to the principle peak. (Note that the area of the side peaks are multiplied with a factor of 3.) This is due to an interference with a four-pulse photon echo (4PE) as described in more detail in the text.

Fig. 2). These higher-order types of echoes have been observed previously and have been denoted virtual echoes [21].

To demonstrate that our PE based measurement setup is analogous to an interferometer for analyzing the time-bin pulses, we also performed visibility measurements using time-bin pulses having different relative amplitudes. As expected, the extracted visibility increases with amplitude ratio and it follows, within the experimental error, the

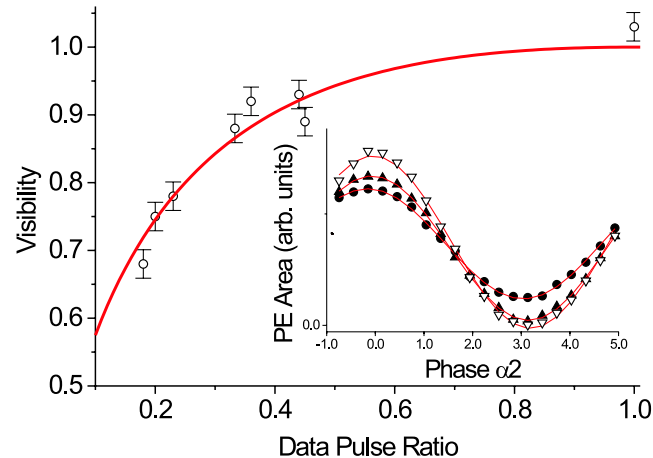


FIG. 3 (color online). The visibility as a function of the ratio between the two time-bin pulses is shown. Experimental points \circ are in good agreement with the theoretical prediction, which contains no free parameter. Inset: The area under the interfering photon echoes is plotted as a function of the phase for different incoming time-bin amplitude ratios (\bullet $V = 0.68$, \blacktriangle $V = 0.93$, ∇ $V = 1.04$). The interference visibility (V) is extracted from a sinusoidal fit.

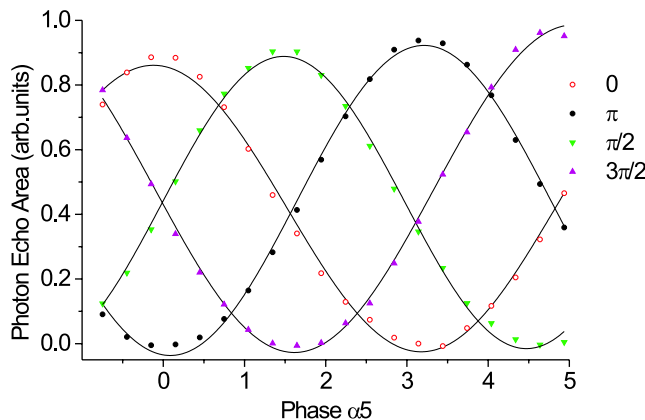


FIG. 4 (color online). Area under the echo as a function of the phase of the second readout pulse. All four classical states, analogous to the quantum states used in four-state quantum cryptography protocols, are stored, retrieved, and analyzed with close to 100% fidelity. This is possible even though the probability of retrieval from the memory is only a few percent, limited by the efficiency of the photon-echo process and by decoherence processes in the storage material.

theoretical relationship (see above). Perfect visibility was reached in the case of equal amplitudes (see Fig. 3). Note that the experimental error is in principle larger for equal time-bin amplitudes, as the method of background subtraction is more sensitive to noise when the photon-echo signal is small, i.e., at the point of destructive interference. The error bars for all depicted data points in Fig. 3 are calculated from standard deviations of a large number of measurements for $R = 1$, setting thus an upper limit.

In Fig. 4 the area under the echo is plotted as a function of the phase α_5 that is applied to the second of the read pulses. While this phase is scanned, the phase α_3 of the time-bin pulse is kept constant at: 0, $\pi/2$, π , and $3\pi/2$ and all other phases are kept at zero. We observed an average visibility of 100% (within the experimental error), corresponding to a fidelity [$F = (1 + V)/2$] close to 100%. This experiment is conceptually analogous to preparing four different time-bin qubits states of two conjugate bases on the equator of the Poincaré sphere, as it is widely used in quantum cryptography in the so-called BB84 [22] or four-state protocol. While in quantum cryptography setups the projection measurement is done with an interferometer [2], we project the state with photon echoes using two read pulses. The photon-echo process thus serves two purposes: storage and retrieval, as well as analysis of the state.

Our results show that the relative phase and amplitude ratio of time-bin pulses can be preserved during storage in the optical memory. Apart from the variation of the visibility due to the change of ratio between the two time-bins, no further reduction is observed, despite the fact that the atomic coherence time is such that a significant part of the atomic coherence is lost during the storage time. This can

be interpreted in the following way: external perturbation of the atomic coherence in the erbium ions reduces the macroscopic dipole moment, representing a loss of coherent ions, which reduces the size of the coherent emission. The ions that have undergone no or small decoherence, however, still retain the phase and amplitude information of the incoming excitation fields, which make it possible to store and retrieve information with high fidelity despite the decoherence in the photon-echo material. This is true as long as the time separations between the time bins is comparable to or smaller than the decoherence time [see Eq. (1)]. Because of the possibility of postselection a nearly perfect fidelity can be obtained, which is promising for a future CRIB based quantum memory [7,9].

This work was supported by the Swiss NCCR Quantum Photonics and by the EU under the Integrated Project Qubit Applications. M. A. acknowledges financial support from the Swedish Research Council and W. T. by iCORE.

*Present address: Institute for Quantum Information Science, University of Calgary, Canada.

- [1] J. Brendel *et al.*, Phys. Rev. Lett. **82**, 2594 (1999).
- [2] N. Gisin *et al.*, Rev. Mod. Phys. **74**, 145 (2002).
- [3] H. J. Briegel *et al.*, Phys. Rev. Lett. **81**, 5932 (1998).
- [4] B. Julsgaard *et al.*, Nature (London) **432**, 482 (2004).
- [5] T. Chanelière *et al.*, Nature (London) **438**, 833 (2005).
- [6] M. D. Eisaman *et al.*, Nature (London) **438**, 837 (2005).
- [7] B. Kraus *et al.*, Phys. Rev. A **73**, 020302(R) (2006).
- [8] A. L. Alexander *et al.*, Phys. Rev. Lett. **96**, 043602 (2006).
- [9] N. Sangouard *et al.*, quant-ph/0611165 [Phys. Rev. A (to be published)].
- [10] A. V. Gorshkov *et al.*, quant-ph/0612084.
- [11] T. W. Mossberg, Opt. Lett. **7**, 77 (1982).
- [12] M. Mitsunaga, Opt. Quantum Electron. **24**, 1137 (1992).
- [13] M. Arend *et al.*, Opt. Lett. **18**, 1789 (1993).
- [14] U. Elman *et al.*, J. Opt. Soc. Am. B **13**, 1905 (1996).
- [15] T. Wang *et al.*, Phys. Rev. A **60**, R757 (1999).
- [16] In the case of a simple 3PE, where the excitation pulses have the phase α_i , $i = 1, 2, 3$, the echo will have the phase $\alpha_e = \alpha_1 - \alpha_2 - \alpha_3$.
- [17] M. U. Staudt *et al.*, Opt. Commun. **266**, 720 (2006).
- [18] I. Baumann *et al.*, Appl. Phys. A **64**, 33 (1997).
- [19] Y. Sun *et al.*, J. Lumin. **98**, 281 (2002).
- [20] The 4PE phase Θ depends on the contributing pulse phases for our configuration for the left and right side peak as follows: $\Theta_1 = \alpha_1 - 2\alpha_2 + \alpha_3 - \alpha_5 + \pi$ and $\Theta_2 = \alpha_1 - \alpha_2 + \alpha_4 - 2\alpha_5 + \pi$. As can be seen in Fig. 2 the dependency of the phase of the side peaks is displaced by π from the principal peak leading into a flip of maximum and minimum.
- [21] Z. Cole, master thesis, Montana State University, Montana, 2000.
- [22] C. H. Bennett and G. Brassard, in *Proceedings of the IEEE International Conference on Computers, Systems and Signal Processing, Bangalore, India* (IEEE, New York, 1984), p. 175.